Fluorescent CsPbBr_3/Cs_4PbBr_6 Nanocomposite Perovskite, Towards Achieving Stability Prospects: Optical Properties, Synthesis Approaches, and Versatile Applications.

Omar, Mohamed
Interdisciplinary Graduate School of Engineering Sciences, Kyushu University

Song, Dongyuan
Interdisciplinary Graduate School of Engineering Sciences, Kyushu University

Taha, Mohamed M.
Department of Chemistry, Faculty of Science, South Valley University

Abdelmonsef, Aboubakr H.
Department of Chemistry, Faculty of Science, South Valley University

他

https://doi.org/10.5109/7395636

出版情報：Proceedings of International Exchange and Innovation Conference on Engineering & Sciences (IEICES). 11, pp.1006-1013, 2025-10-30. International Exchange and Innovation Conference on Engineering & Sciences
バージョン：

Fluorescent $CsPbBr_3/Cs_4PbBr_6$ Nanocomposite Perovskite, Towards Achieving Stability Prospects: Optical Properties, Synthesis Approaches, and Versatile Applications.

Mohamed Omar[1,2], Dongyuan Song[1], Mohamed M. Taha [2], Aboubakr H. Abdelmonsef [2], and Sen Po Yip[3]
[1]Interdisciplinary Graduate School of Engineering Sciences, Kyushu University, 6-1 Kasugakoen, Fukuoka 816-8580, Japan, [2]Department of Chemistry, Faculty of Science, South Valley University, Qena 83523, Egypt, [3]Institute for Materials Chemistry and Engineering, Kyushu University, Fukuoka 8168580, Japan
Corresponding author email: ahmed.mohamed.392@s.kyushu-u.ac.jp

Abstract: *The distinctive superiority of $CsPbBr_3/Cs_4PbBr_6$ nanocomposite perovskite stability had directed the researchers to focus on exploring in-depth of its properties to meet the growing demand for achieving the optimal properties of perovskite for commercial applications. This review aspires to provide a concise summary addressing the most widely fabrication techniques of $CsPbBr_3/Cs_4PbBr_6$ nanocomposite perovskite with touching upon its optical features as well as its applications for a wide range of industrial and commercial sectors. We consider that this review offers a broad perspective of existing obstacles, references for diverse insights of nanocomposite perovskite production and discussion to improve its future usage for various applications.*

Keywords: Ligand assisted reprecipitation; Lead bromide perovskite; Hot injection; Photovoltaic application.

1. INTRODUCTION

Metal halide perovskites (MHPs) are at the forefront of semiconductor materials research, especially in the recent decade, because of their outstanding properties, elemental abundance, and easy to prepare [1], [2]. Despite it had been recognized in 1893 [3], it started to capture the interest of the researchers and engineering communities in 1990s [4] and peaked in the last decade as a result of owing outstanding capacity not just for solar electricity generation but also for light emitting applications. In addition, MHPs exhibit several remarkable features, such as prolong carrier diffusion lengths, high carrier mobility, near-unity photoluminescence quantum yield (PLQY), tunable bandgap with emission across whole visible range, exceptional absorption coefficients, unique defect tolerance, as well as the narrow full width at half maximum (FWHM) for light emission (high color purity) [5], [6]. These extraordinary features make MHPs ideal candidates for lasers and light emitting diodes (LEDs) and transistors, gas sensing of wide range gases, chemical compounds, humidity, temperature, and various photovoltaic and optoelectronic applications [5].

By and large, MHPs are one of the key types of perovskites with general structure formula AMX_3, which represents a cuboidal unit cell where an A cation is located at center with eight corner-sharing $[MX_6]^{4-}$ octahedra surrounding it [7]. Generally, for MHPs, A could be methylammonium (MA), formamidinium (FA), rubidium (Rb) or cesium (Cs). M could be lead (Pb), tin (Sn), or germanium (Ge), and X could be chloride (Cl), bromide (Br), or iodide (I) [8]. The geometry of perovskites is determined by the parameter called the Goldschmidt tolerance factor (t) described in Eq. (1) to estimate the stability of their structures, where rA, rM, and rX are the ionic radii of the ions A, B, and X respectively [9].

$$t = (r_A + r_M) / \sqrt{2}\,(r_A + r_M) \quad (1)$$

Based on the tolerance factor, stable 3D perovskite structures are formed when t value ranges from 0.76 to 1.13; however, if it exceeds or drops below this range a low-dimensional structure type is formed [10]. That is why stable structures of MHPs perovskites can be given by limited number of A cations such as Cs, MA, or FA. Remarkably, the t value for cesium lead bromide is 0.92 that is considered an optimum value for achieving the stability of perovskites and facilitates the stabilization of the perovskite phase in a broader temperature range and improves the thermal stability [11]. As a result of the above, ternary cesium lead bromide ($CsPbBr_3$) is considered the rising star of the industrial world [12].

In this regard, ternary cesium lead bromide lattice can be readily reorganized into different phases as illustrated in figure. 1. The 3D $CsPbBr_3$ structure consists of corner-sharing $[PbBr_6]^{4-}$ octahedra, with the Cs^+ cations occupying the spaces created by the four neighboring $[PbBr_6]^{4-}$ octahedra, resulting in a cubic or pseudo cubic structure. In addition to the $CsPbBr_3$ structure, other types of ternary halide perovskites with minimized structural dimensions and more anisotropic crystal structures such as Ruddlesden-Popper phases (Cs_2PbBr_4), which is composed of 2D sheets of corner-sharing $[PbX_6]^{4-}$ octahedra propagating along the 2D plane. Another 2D version of cesium lead bromide perovskite is represented by $CsPb_2X_5$ that have been exhibited with a tetragonal phase consists of alternating Cs^+ and $[Pb_2X_5]^-$. Additionally, Pb-deficient Cs_4PbBr_6 phase is crystalized in a 0D structure, where $[PbBr_6]^{4-}$ octahedra are completely separated from one another, and the bromide ions are no longer shared among them [5], [7], [13], [14].

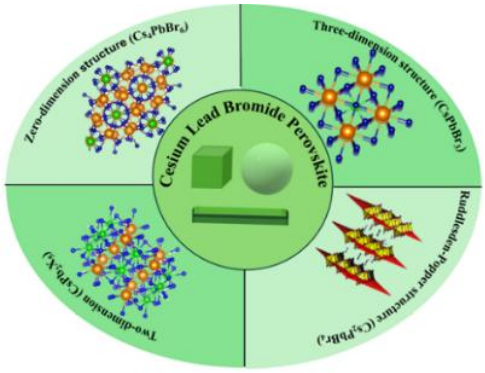

Figure 1. Diagram of different types of ternary cesium lead bromide lattice phases (blue balls, bromine atoms; large orange balls, cesium atoms; green balls, lead atoms). The Ruddlesden-Popper structure (Cs_2PbBr_4) was Reprinted with permission from ref.[14].Copyright 2015, American Chemical Society.

Despite of the intriguing potential of MHPs [5], it is widely known that the environmental instability of MHPs was caused mainly by its soft ionic bonding nature and low crystal lattice energy, leading to not only phase degradation and decomposition, but also poor electron mobility and luminescence quenching which regards a major obstacle that significantly obstructs their growth in practical applications and commercialization [15], [16]. Furthermore, the decline in dimensionality contributes to an increase in the bandgap. For example, 3D $CsPbBr_3$ has a bandgap of 2.36 eV while Cs_4PbBr_6 has a bandgap is ca. 3.95 eV influenced by the electronic decoupling of $[PbBr6]^{4-}$ octahedra [17].

In this regard, over the last two decades, distinguished research contributions have been made to overcome these limitations by proposing solvents and anti-solvents for the synthesis techniques, and the use of specific ligand (monodentate, bidentate) [18]. Despite these techniques being able to somewhat stabilize the crystals and the photoluminescence (PL), achieving colloidal stability under more extreme conditions was still under investigation [19]. With the aim of achieving stabilization, post synthetic modifications using surface passivation or encapsulation techniques were conducted [20], [21]. The stability of $CsPbBr_3$ perovskites has been significantly enhanced by using mesoporous materials [22], inorganic oxides [23], polymer matrixes [24], and last but not the least, inert shells such as (SiO_2, ZnS, CdS and Cs_4PbBr_6) [25]. Recent studies indicate that $CsPbBr_3/Cs_4PbBr_6$ heterostructure has outstanding stability and high PLQY, where utilizing the wide bandgap Cs_4PbBr_6 matrix to cover the $CsPbBr_3$ lead to improve the optical-electrical properties by confining carriers to the $CsPbBr_3$ region and reducing the probability of electron leakage [26], [27].

Historically $CsPbBr_3$ and Cs_4PbBr_6 were reported for the first time in 1893, when Wells and his colleagues synthesized both in the aqueous solution [28]. Then Kristallogr.et.al investigated the crystal structure, photoconductivity and synthesis of $CsPbBr_3$ that had been distinguished by orange color whereas Cs_4PbBr_6 particles are colorless [29]. Afterward, Zeng. et. al. and Kovalenko and coworkers synthesized $CsPbBr_3$ quantum dot with high photoluminescence quantum yield (PLQY) to achieve higher stability and considerable potential in optoelectronic applications [12], [30]. Despite the $CsPbBr_3$'s merits over hybrid and inorganic halide perovskites [31], it is not exaggeration to say that the instability of $CsPbBr_3$ nanoparticles in ambient temperature was an impediment for commercial application [32]. Although the stability that enhanced by introducing $CsPbBr_3/Cs_4PbBr_6$ composite, the availability of literature reviews with comprehensive discussions about synthesis approach, properties and commercial applications are limited.

Drawing inspiration by the forementioned, this review aims to summarize the nature, and optical properties of $CsPbBr_3/Cs_4PbBr_6$ nanocomposite and provide perspective into the origination of fluorescence. On the other hand, we come through the parameters that affect the formation of nanocomposite and fabrication methods over the past five years by paying special attention to colloidal-based synthesis approaches. Finally, we discussed briefly their potential industrial utilization across diverse sectors such as light emitting diode, solar cell, sensing, anticounterfeiting, photodetector, and photocatalysis applications.

2. OPTICAL PROPERTIES OF $CsPbBr_3/Cs_4PbBr_6$ NANOPARTICLES.

It's widely acknowledged that tuning the structures and morphologies of perovskite has a strong influence to achieve superb optical and photochemical performance [33], [34]. In accordance with that $CsPbBr_3$ nanocrystals with tunable bandgap are obtainable in various morphologies (nanocubes, nanorods (NRs), nanowires (NWs), and nanospheres) by manipulating the amount of solvent, ligand concentration, and reaction temperature which contribute to the high PLQY as well as narrow emission widths and tunable mobility of charge-transport of $CsPbBr_3$ nanocrystals providing it with excellent optical properties [35]. Due to certain drawbacks of $CsPbBr_3$ nanocrystals, including sensitivity against moisture, heat, and decrease in PLQY over time, extensive research efforts have been devoted to synthesizing $CsPbBr_3/Cs_4PbBr_6$ composites which are known for their significant enhancement in luminescence and stability. Despite the $CsPbBr_3/Cs_4PbBr_6$ composites typically present in a bulk form in absence of quantum confinement effect, they still maintain a strong bright fluorescence, which is considered a promising approach to address the instability issue [36]. Despite the researchers have demonstrated that the intriguing stability of Cs_4PbBr_6 against temperature, water, UV radiation, and humidity [37], the origin of the luminescence mechanism for Cs_4PbBr_6 is still under debate [38]. Several explanations had been proposed regarding the origination of the optical performance of $CsPbBr_3/Cs_4PbBr_6$ perovskite, that can be summarized into the following two hypotheses: defect-state which manifest in bromide vacancies, and coexistence of $CsPbBr_3$ nanoparticles [36], [39], [40]. By and large, bromide vacancies represent the most commonly found defect states in perovskites that had been verified by various experiments [41], [42], where the defect state (bromide vacancies) of emissive perovskites was verified by monitoring the appearance of Urbach tail in absorption spectra. Conversely, no Urbach tail in absorption was observed for nonemissive perovskite. These experimental findings proves that bromide vacancies as an origin of fluorescence in perovskite [43].

Despite other lattice defects being proposed like interstitial water molecules, these defects were not verified experimentally to these days [44]. On the other hand, the presence of $CsPbBr_3$ as a byproduct during synthesis of pure 0D Cs_4PbBr_6 shows the same influence of the Urbach tail on the absorption. Notwithstanding the existence of these byproducts in 0D Cs_4PbBr_6 had not been evidenced by characterization techniques (such as XRD and TEM), the ion exchange reactions address evidence to support the coexistence of $CsPbBr_3$ in 0D Cs_4PbBr_6 where the halogen exchange reaction occurs smoothly with $CsPbBr_3$, whereas it fails with Cs_4PbBr_6 because of isolation of $[PbBr_6]$ units by sublattice of Cs^+ ions [45].

Regardless of the origin of the fluorescent in perovskite composite, it is worth to mention that it has high PLQY with narrow FWHM and strong PL emission which promotes the optical performance as well as the outstanding enhancement of thermal/photo stability for $CsPbBr_3/Cs_4PbBr_6$ crystals compared to standalone $CsPbBr_3$, make them promising to apply in wide range of technologies [46] as will be discussed in section 4.

3. SYNTHESIS OF $CsPbBr_3/Cs_4PbBr_6$ NANOPARTICLES.

Among all types of approaches for synthesis of MHPs it had been proven that the liquid phase is considered the superior strategy [47]. At the same time different techniques involving saponification approach [48], low-temperature ligand-assisted reprecipitation (LARP) method [49], microwave assisted method, conventional heating (CH) methods [50], hot injection method [51] and solvothermal synthesis method [52] have been utilized for fabrication of $CsPbBr_3/Cs_4PbBr_6$ perovskite composites. In this review, we will focus on the reports for synthesizing $CsPbBr_3/Cs_4PbBr_6$ composite in the last five years.

To investigate the stability of $CsPbBr_3/Cs_4PbBr_6$ composite, Bao and coworkers synthesized $CsPbBr_3/Cs_4PbBr_6$ nanocrystals around 13.9 nm via hot injection method by adding $SnBr_2$ to lead bromide solution as an outstanding modification to partly replace lead ions in the precursor and produce extra bromide ions resulting in promotion of $CsPbBr_3/Cs_4PbBr_6$ nanocomposite formation. A highly efficient nanocomposite with pure single phase was fabricated by optimizing the synthesis condition through using different amount of $SnBr_2$ and different reaction temperatures. Of note, the passivation of $CsPbBr_3$ utilizing Cs_4PbBr_6 crystals caused a downturn trion formation, PLQY enhancement, and reduced crystal defects revealing the outstanding potential [51]. Within the same year, Peng et al. conducted a comprehensive study of the $CsPbBr_3/Cs_4PbBr_6$ composite synthesized by hot injection method. The $CsPbBr_3/Cs_4PbBr_6$ composite, with approximately 10 nm as average size, was synthesized using where cesium carbonate, and lead bromide were heating under nitrogen atmosphere in 10 ml of 1-octadecene that congaing oleic acid and oleyl amine as capping agents. The composite shows a ~57 % of PLQY. In their report, the reaction time was fixed at 20 min, while different temperatures were tested to assess the performance of the composite (60–110℃). The authors noted that the composite emission is tunable with varying the temperature giving the maximum PL emission with narrow linewidth of (22nm) at 90 ℃ [53]. The $Cs_4PbBr_6/CsPbBr_3$ nanocomposite can be used for light emitting diode (LED) applications. Huang et al. demonstrated a facile approach for the synthesis of luminescent $Cs_4PbBr_6/CsPbBr_3$ nanocomposite with production yield 90% and quantum yield reaches up to 85%, by antisolvent-assisted transformation of $CsPbBr_3$ powder as demonstrated in figure (2). The antisolvent (toluene, m-xylene, chloroform, and acetonitrile) was added to 1 ml DMSO containing CsBr and $CsPbBr_3$ powder in different ratios (1:1, 4:1, 6:1, and 8:1) to produce $Cs_4PbBr_6/CsPbBr_3$ nanocomposite. The method demonstrated a significant improved production yield and the nanocomposite demonstrated high PLQY, notable resistance against air and humidity made it a valuable candidate for optoelectronic applications [54].

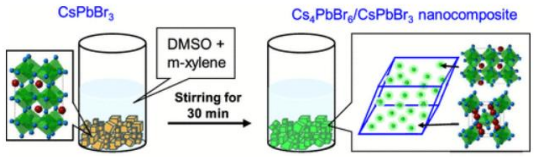

Figure 1. Antisolvent-assisted approach for synthesis of $Cs_4PbBr_6/CsPbBr_3$ nanocomposite. Reprinted with permission from ref. [54]. Copyright 2020, American Chemical Society.

Li et al. reported a facile approach of in-situ synthesis of polymers contained $Cs_4PbBr_6/CsPbBr_3$ nanocomposite to achieve the utmost level of photostability, and the water stability of $CsPbBr_3$ enables it to be used for liquid crystal display backlight. In short, the nanocomposite was synthesized by supersaturated recrystallization method at room temperature, employing Cs_4PbBr_6 and polymethylmethacrylate as dual protection to enhance the performance of $CsPbBr_3$, resulting in a $Cs_4PbBr_6/CsPbBr_3$ nanocrystals with characteristic green photoluminescence peak centered at 518 nm, PLQY reached over 85%, and full width at half maximum (FWHM) at around 19 nm [27]. To examine the origin of green emissions in $Cs_4PbBr_6/CsPbBr_3$ nanocomposite, Bao and his colleagues made a comparison between the PL behavior of imbedded $CsPbBr_3$ nanoparticle within Cs_4PbBr_6 as inert host and pure $CsPbBr_3$ that had been fabricated utilizing hot injection method. The authors revealed that despite the synchrotron XRD data showing only the Cs_4PbBr_6 phase existed in the sample, the high-resolution transmission electron microscope (HRTEM) revealed beyond doubt that the existence of many $CsPbBr_3$ quantum dots with average size 3.8 nm in the Cs_4PbBr_6 crystals, as depicted in figure (3a and b) [55].

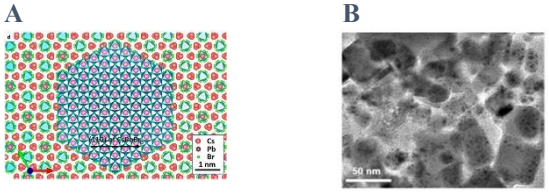

Fig. 2. (a) Model exhibits an embedded $CsPbBr_3$ nanoparticle within the Cs_4PbBr_6 host lattice. (b) TEM image of Cs_4PbBr_6 crystals with dark dots of embedded CsPbBr3 crystals. The two Reprinted with permission from ref. [55] Copyright 2020, American Chemical Society.

Altaf et al. introduced the deposition of $Cs_4PbBr_6/CsPbBr_3$ nanocomposite on 3D-ZnO thin film seeking to enhance the emission properties of ZnO in luminescence-based applications. Synthesis and deposition of the nanocomposite has been achieved through spin coating method. In this method, a preheated ZnO thin film at 80 ◦C was rotated at 3000 rpm. Specific concentrations of $PbBr_2$ in DMF and CsBr in isopropanol were subsequently spin-coated on the ZnO thin film and followed by annealing for 10 min at 280 ◦C to produce $Cs_4PbBr_6/CsPbBr_3$ nanocomposite on ZnO film. The findings provided that an exceptional enhancement in the luminescence intensity of dual $Cs_4PbBr_6/CsPbBr_3$ nanocomposite system compared to $CsPbBr_3$ system is revealed. Finally, by studying the stability against air and humidity of the thin films, it was proved that the perovskite nanocomposite-ZnO film exhibits superior stability in ambient atmosphere for at least 7 weeks[56] . Aiming to obtain solid $CsPbBr_3$ QDs with high stability and PLQY, Wang and his group applied self-assembly technique for fabrication of $CsPbBr_3/Cs_4PbBr_6$ nanocomposite and reported its effectiveness against counterfeiting. Briefly, the nanocomposite was prepared by stirring various ratio of CsBr: PbBr2 (1, 2, 4, 6, and 6.5) in mixture of DMF, DMSO, oleic acid and oleyl amine at room temperature. Afterwards the temperature was raised in parallel with injection an aqueous solution of HBr (0.1 ml) under influence of stirring and heating for 10–15 as illustrated in figure (4). The prepared $Cs_4PbBr_6/CsPbBr_3$ in the different molar ratios were green light emitting and all the samples exhibiting nearly identical XRD patterns. Motivated by previous findings, the authors carried out a stability comparison among $Cs_4PbBr_6/CsPbBr_3$, $CsPbBr_3/SiO_2$, and $CsPbBr_3$ QDs by monitoring the PL intensity after storing for two month under ambient conditions and after heating up to 100 °C, where $Cs_4PbBr_6/CsPbBr_3$ demonstrated significant superiority in the stability compared to the other composites by maintain about 90% and 80% of its PLQY after two month of saving under ambient conditions or 24 h heating respectively, as reflected in figure(5 a and b) [57].

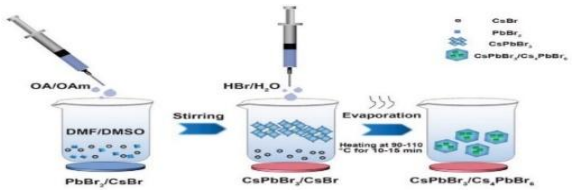

Fig. 3. Illustration of low-temperature self-assembly technique for the CsPbBr3/Cs4PbBr6 nanocomposite fabrication. Reprinted with permission from ref [57]. Copyright © 2021 John Wiley & Sons.

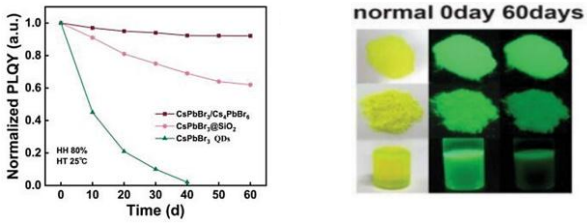

Fig. 5. a PLQY of the $CsPbBr_3/Cs_4PbBr_6$ nanocomposite, $CsPbBr_3@SiO_2$ and $CsPbBr_3$ QDs after 60 d of storage under ambient condition. an Optical images under sunlight and UV irradiation of the $CsPbBr_3/Cs_4PbBr_6$ nanocomposite, $CsPbBr_3@SiO_2$ and $CsPbBr_3$ QDs after 60 d of storage under ambient condition. The pictures were Reprinted with permission from ref.[57]. Copyright © 2021 John Wiley & Sons.

Fonseca and co-workers developed a strategy based on hot injection method to enhance the optical stability of (3D) $CsPbBr_3$ nanocrystal surface via a (0D) Cs_4PbBr_6 shell in presence of different polar solvents and diverse composition to achieve the optimized surface passivation and limited the nonradiative pathways. When in inert atmosphere, a heated solution of cesium carbonate Cs_2CO_3 in 1-octadecene (ODE) and oleic acid (OA) was rapidly injected into a three-neck flask containing $PbBr_2$, OA, and oleylamine (OAm) dissolved in 5 mL of ODE to produce a colloidal solution of $Cs_4PbBr_6/CsPbBr_3$ nanocomposite. In the latter part of the study, the 0D/3D core/shell sample was post-treated by isopropanol or ethyl acetate as antisolvents to control the surface. After that, the obtained solid sample was exhaustively examined as promising enhanced PLQY, stability and surface passivation compared to the 3D sample. These capabilities establish it as an excellent choice for photovoltaic or photoelectrochemical applications [58]. Microwave assisted heating technique was reported by Lu and coworkers to prepare $CsPbBr_3$ /Cs_4PbBr_6 composites with improved PLQY compared to conventional heating methods. The process included dissolving $PbBr_2$ and CsBr as precursor for perovskites fabrication in a specific volume of dimethyl sulfoxide. The mixture was then stirred for 5 min after adding OA and tetraoctylammonium bromide as ligands. After that, the mixture was added drop-by-drop to poor solvent such as tert-butanol and/or toluene, the obtained colloidal solution undergoes heating via microwave irradiation for 5–45 min to produce yellow powder of $CsPbBr_3/Cs_4PbBr_6$ [59]. He et al. managed to propose an approach to overcome the instability issue of perovskite nanocrystals through fabrication of ultra-stable $Cs_4PbBr_6/CsPbBr_3$ perovskites that's covered by polyvinyl butyral (PVB) film with excellent optical properties and good heat and water stability. In preparation procedures, CsBr and $PbBr_2$ (6:1) were stirred in 12 ml DMF solution containing OA and OAm at 90 ◦C to produce precipitate of Cs_4PbBr_6 /$CsPbBr_3$ perovskites. Subsequently, various weights of the perovskites (0.1, 0.3, 0.5, 0.8, and 1.0 mg) were added to colloidal solution of PVB in chloroform with various stirring. A series of HPSs@PVB membrane shaped with double shieling was produced as shown in [60]. In 2022, Naresh and coworkers used eco-friendly ultrasonication techniques for ligand-free fabrication of $Cs_4PbBr_6/CsPbBr_3$ microcrystals (MCs), exhibiting an improved PLQY and overcoming stability limitations. The synthesis of MCs involved a single-step room temperature process in which CsBr and $PbBr_2$ were taken in 4:1 molar ratio and ultrasonicated in equivalent amounts of DMF/DMSO for 30 min to produce MCs with a yellow color after centrifugation. The dual phase structure of MCs was confirmed by XRD and SEM which validated the $CsPbBr_3$ crystals that are embedded into the Cs_4PbBr_6 [61]. Babeker et al. reported a multiple protection of unstable $CsPbBr_3$ quantum dots through combining specific amounts of Cs_2CO_3, $PbBr_2$, sodium bromide (NaBr), silicon dioxide (SiO_2), boron oxide (B_2O_3), and lithium carbonate (Li_2CO_3). The mixture was then sintered in an alumina crucible for 30 min at 1100

◦C. Finally, by employing molten glass, the authors managed to produce a glass sample containing $Cs_4PbBr_6/CsPbBr_3$ QDs embedded in lithium borosilicate, confirmed by XRD. The sample showed extraordinary stability in water for 30 days [62]. Ming and others managed to obtain an orange precipitate of Cs_4PbBr_6/ $CsPbBr_3$ polycrystalline composites via solution of $PbBr_2$ in DMSO, which was mixed under stirring with CsBr solution prepared by dissolving Cs_2CO_3 in a 5 ml of concentrated HBr. Then 10 ml of DMSO was added to the stirred solution in parallel with heating to 55 ◦C followed by cooling. Finaly, the heating and cooling process was repeated until a bright green precipitate was produced at the bottom of the solution that owns good optical and thermal properties [63].

Qian and his research group has reported a mechanosynthesis approach for improving the emission intensity, PLQY and photoluminescence properties of $CsPbBr_3$ powder via successive grinding the powder of $CsPbBr_3$, which resulting from dissolving equal molar of CsBr and $PbBr_2$ in DMSO under continuous stirring in ambient air with excessive amount of CsBr powder with ratio 1:0, 1:1, 1:3, 1:5, and 1:7, respectively, to give $Cs_4PbBr_6/CsPbBr_3$ powder with outstanding optical and thermal properties[64]. In a comparable manner, with advantage of avoiding ligand and antisolvent usage, Rao et al. address the instability of $CsPbBr_3$ by utilizing the high-speed mechanical mixing strategy under ambient atmosphere to form a heterostructure of $Cs_4PbBr_6/CsPbBr_3$ in which $CsPbBr_3$ was imbedded in Cs_4PbBr_6 as a large bandgap matrix. In a typical synthesis, a 1:4 molar ratio of $PbBr_2$ and CsBr were placed in bottle containing 2.5ml of DMSO subspecialty. The sample was grounded continuously in an automatic mixer for 1 h. Finally, a yellow powder of $Cs_4PbBr_6/CsPbBr_3$ was obtained by vacuum filtration. This synthesis process is repeated in eight glass bottles to achieve large scale production [36]. In addition to this work, the same research group pursued another eco-friendly method with the aid of liquid paraffin and ultrasonication for fabrication of $CsPbBr_3/Cs_4PbBr_6$ composites with strong emission and high stability. The authors improved the previous preparation method to reduce the polar solvent usage alongside avoiding ligands and antisolvents, where both of CsBr and $PbBr_2$ were sonicated for 30 min in 4 ml of paraffin/DMSO solvent mixture. Subsequently, the residual was purified by removing unreacted precursor through centrifugation to produce green emitting powder. The dual protection of $CsPbBr_3$ by paraffin oil and Cs_4PbBr_6 had a positive effect on the significant photostability, thermostability and polar solvent stability of $CsPbBr_3$/Cs4$PbBr_6$ composites in contrast to CsPbBr3 and $CsPbBr_3/Cs_4PbBr_6$ that obtained in absence of paraffin oil [65].

Properties and formation mechanism of $CsPbBr_3$ embedded in Cs_4PbBr_6 were reported by Sun and coworkers, who prepared $CsPbBr_3$/Cs4$PbBr_6$ composites via different ratios of precursors (CsBr and $PbBr_2$). The authors employed an antisolvent precipitation method where the precursors were added to a combination of DMSO and DMF containing OA and OAm as ligand as well as 2-methyl imidazole (MeIm). The solution was stirred for one hour followed by adding a portion of the solution to 10 ml of antisolvent (toluene) to produce light green suspension solution. Under the influence of additional toluene, solid precipitate of core-shell $CsPbBr_3/Cs_4PbBr_6$ was obtained after purification of ligands and MeIm[66]. Relying on inverse microemulsion method at ambient conditions, core/shell $CsPbBr_3/Cs_4PbBr_6$ and $CsPbBr_3$ nanocrystals were managed to be obtained by manipulating the ratio of cesium and lead sources. Cesium-oleate precursor was prepared first by stirring Cs_2CO_3 in about 11 ml of OA in nitrogen atmosphere. Then, 50 μL of Cs-oleate precursor was added to hexane and a small amount of OA under influence of stirring, heating and degassing which evacuate moisture and oxygen. Afterward, a DMF solution, acidified with HBr, containing $PbBr_2$, OA, and OAm, was drowsily added to the former Cesium-oleate solution under various stirring. 10 min later a green powder of $CsPbBr_3$ /Cs_4PbBr_6 core/shell was obtained by centrifugation [67].

4. APPLICATIONS OF $CsPbBr_3/Cs_4PbBr_6$ NANOPARTICLES.

Whereas the passivation of unstable surface of $CsPbBr_3$ particles and inhibiting its agglomeration and regrowth was successfully achieved by Cs_4PbBr_6, the upcoming step will be the investigation the degree of efficacy for $CsPbBr_3/Cs_4PbBr_6$ heterostructure on a broad scale of practical applications including light emitting diodes, solar cells, photodetectors, photocatalysis, sensors, and anticounterfeiting applications.

It is found that the $CsPbBr_3/Cs_4PbBr_6$ heterostructure is a promising candidate for white light emitting diode (LED) application [36], [65], [68]. Wang group had fabricated a white LED through mixing powder of $Cs_4PbBr_6/CsPbBr_3$ millimeter-scale crystals with silicone gel that contains $K_2SiF_6:Mn^{4+}$ (KSF). The mixture was applied on a 450 nm substrate as blue emitting sources. The LED device obtained showed a color coordinate under 20 mA, almost equal to the standard white color coordinate. Moreover, the National Television Systems Committee (NTSC) standard was surpassed by the device's color gamut, which is measured at 128.66% while the luminous efficiency of the device is 64.56 lm/W. Finally, a high Correlated Color Temperature (CCT) stability was observed by the electroluminescence (EL) spectra for gradually changed working current from 5 to 100 mA[68].

In another study of the liquid paraffin-based $CsPbBr_3/Cs_4PbBr_6$ white LED device, not only outstanding luminescent performance was achieved with a power efficiency of 129.5 lm/W and a broad color gamut, covering 121% of the NTSC, but also the investigation the potential of visible light communication (VLC) for the $CsPbBr_3/Cs_4PbBr_6$-LP white LED proved its high performance in high-definition display as well as VLC applications [65].

In order to push for commercial application as a color conversion film, the stability of the prepared $Cs_4PbBr_6/CsPbBr_3$/PMMA film towards water and radiation, emission change was investigated via PLQY to ensure stability. A comprehensive comparison between $Cs_4PbBr_6/CsPbBr_3$/PMMA and $CsPbBr_3$@PMMA revealed that the former exhibited significant green fluorescence stability after immersed in water for a month. On the other hand, $CsPbBr_3$@PMMA suffered from a rapid drop in PLQY. In addition, the photostability test and fluorescence lifetime decay clearly illustrated the superior performance of Cs_4PbBr_6/

$CsPbBr_3$/PMMA compared to $CsPbBr_3$@PMMA. These stability properties give compelling evidence of the suitability of Cs_4PbBr_6/$CsPbBr_3$/PMMA for LCD back lights [27].

Although perovskite-based solar cells presented high performance compared to traditional silicon solar cells,[69] commercial applications are still under development due to the instability [70]. In this regard, researchers dedicated great effort to improve the device performance and its applicability [69], [71], [72], [73]. Meanwhile, a comprehensive study for a composite containing $CsPbBr_3$/Cs_4PbBr_6 QD to form a downshifting composite film to enhance the performance of silicon solar cell. This composite reduced the absorption edge to about 500 nm and hence increased silicon solar cells efficiency by 1.18% which relieved a viral role for perovskite composite in solar cell enhancement [74].On the other hand, Cao et al. managed to use HI-prepared $CsPbBr_3$ and Cs_4PbBr_6 perovskite layers to improve the stability and the efficiency of solar cell device where the presence of perovskite enhanced the voltage, stability, and the photoelectric conversion efficiency (PCE) [73]. Generally, the sensitivity of perovskite against moisture, temperature, and volatile organic compounds was qualified to take the lead in wide range of sensing and anti-counterfeiting applications [75], [76], [77], [78], [79]. One outstanding sensing study was carried out using water stable $CsPbBr_3$/Cs_4PbBr_6 composite with strong green fluorescence (525 nm) for sensing of folic acid (FA), where a solution of perovskite in ultrapure water was subjected to wide range of FA concentration as well as other small biomolecules. The experiments proved the ability of FA to quench the fluorescence intensity which is linearly proportional to the FA concentration in the range of 10–800 µM. Also, high selectivity of FA relative to other biomolecules is also demonstrated, as shown in figure(6a and b)[75].

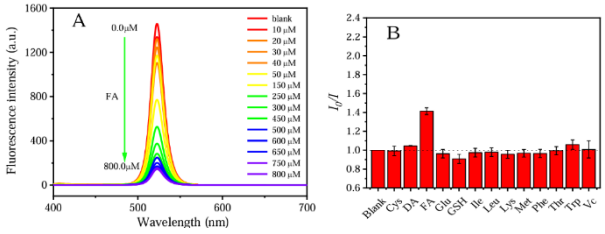

Fig. 6. (a) fluorescence intensity variation as a function of folic acid concentration. (b) selectivity of folic acid relative to other biomolecules. The two pictures were repented by ref [75]. W. Z. She et al., "Selective Detection of Folic Acid Using a Water-Stable Fluorescent CsPbBr3/Cs4PbBr6 Perovskite Nanocrystal Probe," Chemosensors, vol. 11, no. 1, Jan. 2023, doi: 10.3390/chemosensors11010019.

In the same regard, a stable nanocomposite encapsulation in silica microspheres, $CsPbBr_3$/Cs_4PbBr_6/SiO_2 films, was utilized as an anticounterfeiting tool. This phenomenon is attributed to its high sensitivity and fast response to heating, UV and IR light irradiation where $CsPbBr_3$ proved its suitability for anti-counterfeiting applications while both Cs_4PbBr_6 and SiO_2 safeguarding it against moisture, temperature and so on [79]. $CsPbBr_3$@Cs_4PbBr_6-based polymer nanocomposite also exhibited a significant sensitivity against UV radiation [80]. Besides, Han et al. managed to produce a photodetector (PD) based on $CsPbBr_3$/Cs_4PbBr_6 nanocomposites which was regarded as one of the top-tier PDs based on all-inorganic perovskites. The measured detectivity of the PD under 532 nm illumination reached 4.24 Jones which represents a good guidance for developing PDs [81].

Due to the extraordinary light absorption features, physicochemical properties, and fast carrier kinetics of all-inorganic halide perovskite, utilization of different composites of perovskite including $CsPbBr_3$/Cs_4PbBr_6 had gathered momentum as a potential photocatalysts [1], [82], [83]. Accordingly, ligand-assisted precipitation (LARP)-based $CsPbBr_3$/Cs_4PbBr_6 nanosheets were employed to achieve oxidative conversion of styrene into benzaldehyde through photocatalytic mechanism in visible-light. The pristine perovskite nanosheets managed to achieve oxidation rate (372 µmol g−1 h−1) while modification of nanosheets surface via adding $ZrCl_4$ largely improved the photocatalytic oxidation nearly twofold [82].

5. CONCLUSION.

$CsPbBr_3$/Cs_4PbBr_6 heterostructure perovskites have gained remarkable attention due to their significant stability and optical properties. $CsPbBr_3$ provides high PLQY and controllable bandgaps However, its stability under environmental conditions remains an obstacle. In this regard using Cs_4PbBr_6 has enabled to enhance stability without deteriorating the optical performance. In this review, we described the synthesis methods, optical characteristics, and structural aspects of nanocomposites, with a focus on colloidal production techniques. Additionally, their potential industrial uses, such as LEDs, solar cells, and sensors, were addressed. Given the limited reviews on this area, this paper provides insights into its commercialization possibilities and future research prospects.

6. REFERENCES.

[1] A. Thanetchaiyakup et al., "Metal Halide Perovskites for Photocatalysis: Performance and Mechanistic Studies," Chem Asian J, vol. 19, no. 24, Dec. 2024, doi: 10.1002/asia.202400787.

[2] M. A. Green, A. Ho-Baillie, and H. J. Snaith, "The emergence of perovskite solar cells," 2014, Nature Publishing Group. doi: 10.1038/nphoton.2014.134.

[3] V. H. L Wells, "Uber die Casium-und Kalium-Blei halogenide."

[4] V. Ctor Luañ, A. Costales, and A. Martí N Pendá, "Ions in crystals: The topology of the electron density in ionic materials. II. The cubic alkali halide perovskites," 1997.

[5] J. Shamsi, A. S. Urban, M. Imran, L. De Trizio, and L. Manna, "Metal Halide Perovskite Nanocrystals: Synthesis, Post-Synthesis Modifications, and Their Optical Properties," Chem Rev, vol. 119, no. 5, pp. 3296–3348, Mar. 2019, doi: 10.1021/acs.chemrev.8b00644.

[6] Q. Van Le, K. Hong, H. W. Jang, and S. Y. Kim, "Halide Perovskite Quantum Dots for Light-Emitting Diodes: Properties, Synthesis, Applications, and Outlooks," Dec. 01, 2018, Blackwell Publishing Ltd. doi: 10.1002/aelm.201800335.

[7] B. Saparov and D. B. Mitzi, "Organic-Inorganic Perovskites: Structural Versatility for Functional Materials Design," Apr. 27, 2016, American Chemical Society. doi: 10.1021/acs.chemrev.5b00715.

[8] Q. A. Akkerman, G. Rainò, M. V. Kovalenko, and L. Manna, "Genesis, challenges and opportunities for colloidal lead halide perovskite nanocrystals," Nat Mater, vol. 17, no. 5, pp. 394–405, May 2018, doi: 10.1038/s41563-018-0018-4.

[9] Y. Wei, Z. Cheng, and J. Lin, "An overview on enhancing the stability of lead halide perovskite quantum dots and their applications in phosphor-converted LEDs," Jan. 07, 2019, Royal Society of Chemistry. doi: 10.1039/c8cs00740c.

[10] W. Travis, E. N. K. Glover, H. Bronstein, D. O. Scanlon, and R. G. Palgrave, "On the application of the tolerance factor to inorganic and hybrid halide perovskites: A revised system," Chem Sci, vol. 7, no. 7, pp. 4548–4556, 2016, doi: 10.1039/c5sc04845a.
[11] R. X. Yang, J. M. Skelton, E. L. Da Silva, J. M. Frost, and A. Walsh, "Spontaneous octahedral tilting in the cubic inorganic cesium halide perovskites CsSnX3 and CsPbX3 (X = F, Cl, Br, I)," Journal of Physical Chemistry Letters, vol. 8, no. 19, pp. 4720–4726, Oct. 2017, doi: 10.1021/acs.jpclett.7b02423.
[12] J. Song, J. Li, X. Li, L. Xu, Y. Dong, and H. Zeng, "Quantum Dot Light-Emitting Diodes Based on Inorganic Perovskite Cesium Lead Halides (CsPbX3)," Advanced Materials, vol. 27, no. 44, pp. 7162–7167, Nov. 2015, doi: 10.1002/adma.201502567.
[13] L. Dou et al., "Atomically thin two-dimensional organic-inorganic hybrid perovskites," Science (1979), vol. 349, no. 6255, pp. 1518–1521, Sep. 2015, doi: 10.1126/science.aac7660.
[14] D. H. Cao, C. C. Stoumpos, O. K. Farha, J. T. Hupp, and M. G. Kanatzidis, "2D Homologous Perovskites as Light-Absorbing Materials for Solar Cell Applications," J Am Chem Soc, vol. 137, no. 24, pp. 7843–7850, Jun. 2015, doi: 10.1021/jacs.5b03796.
[15] Y. Wei, Z. Cheng, and J. Lin, "An overview on enhancing the stability of lead halide perovskite quantum dots and their applications in phosphor-converted LEDs," Jan. 07, 2019, Royal Society of Chemistry. doi: 10.1039/c8cs00740c.
[16] H. Tian, Y. Liu, and F. L. Jiang, "Chemical Instability of CsPbBr3 Nanocrystals and the Reversible Transformation between CsPbBr3 and Cs4PbBr6 Nanocrystals as Driven by Synthetic Precursors," Chemistry of Materials, 2024, doi: 10.1021/acs.chemmater.4c02018.
[17] B. Kang and K. Biswas, "Exploring Polaronic, Excitonic Structures and Luminescence in Cs4PbBr6/CsPbBr3," Journal of Physical Chemistry Letters, vol. 9, no. 4, pp. 830–836, Feb. 2018, doi: 10.1021/acs.jpclett.7b03333.
[18] M. Kazes, T. Udayabhaskararao, S. Dey, and D. Oron, "Effect of Surface Ligands in Perovskite Nanocrystals: Extending in and Reaching out," Acc Chem Res, vol. 54, no. 6, pp. 1409–1418, Mar. 2021, doi: 10.1021/acs.accounts.0c00712.
[19] L. De Trizio, I. Infante, and L. Manna, "Surface Chemistry of Lead Halide Perovskite Colloidal Nanocrystals," Acc Chem Res, vol. 56, no. 13, pp. 1815–1825, Jul. 2023, doi: 10.1021/acs.accounts.3c00174.
[20] B. Chen, P. N. Rudd, S. Yang, Y. Yuan, and J. Huang, "Imperfections and their passivation in halide perovskite solar cells," Jul. 21, 2019, Royal Society of Chemistry. doi: 10.1039/c8cs00853a.
[21] W. Lv et al., "Improving the Stability of Metal Halide Perovskite Quantum Dots by Encapsulation," Jul. 12, 2019, Wiley-VCH Verlag. doi: 10.1002/adma.201900682.
[22] A. Rubino, L. Caliò, A. García-Bennett, M. E. Calvo, and H. Míguez, "Mesoporous Matrices as Hosts for Metal Halide Perovskite Nanocrystals," May 01, 2020, Wiley-VCH Verlag. doi: 10.1002/adom.201901868.
[23] S. Samiei, E. Soheyli, K. Vighnesh, G. Nabiyouni, and A. L. Rogach, "Exploring CsPbX3 (X = Cl, Br, I) Perovskite Nanocrystals in Amorphous Oxide Glasses: Innovations in Fabrication and Applications," Apr. 25, 2024, John Wiley and Sons Inc. doi: 10.1002/smll.202307972.
[24] S. Liang et al., "Recent Advances in Synthesis, Properties, and Applications of Metal Halide Perovskite Nanocrystals/Polymer Nanocomposites," Dec. 01, 2021, John Wiley and Sons Inc. doi: 10.1002/adma.202005888.
[25] C. Zhang et al., "Core/Shell Metal Halide Perovskite Nanocrystals for Optoelectronic Applications," May 01, 2021, John Wiley and Sons Inc. doi: 10.1002/adfm.202100438.
[26] W. Sun, Y. T. Hung, W. T. Huang, R. S. Liu, and W. Zhou, "Photoluminescent Nano-CsPbBr3 Embedded in Cs4PbBr6 Crystals: Formation Mechanism and Properties," Cryst Growth Des, vol. 24, no. 1, pp. 545–553, Jan. 2024, doi: 10.1021/acs.cgd.3c01226.
[27] X. Li et al., "Facile In Situ Fabrication of Cs4PbBr6/CsPbBr3 Nanocomposite Containing Polymer Films for Ultrawide Color Gamut Displays," Adv Opt Mater, vol. 8, no. 13, Jul. 2020, doi: 10.1002/adom.202000232.
[28] H. L. Wells, "Über die Cäsium- und Kalium-Bleihalogenide," Zeitschrift für anorganische Chemie, vol. 3, no. 1, pp. 195–210, 1893, doi: 10.1002/zaac.18930030124.
[29] W. A. Wooster and C. K. M, "Crystal Structure and Photoconductivity of Caesium Plumbohalides Nuclear Magnetic Resonance in ~-Brass," 1936.
[30] L. Protesescu et al., "Nanocrystals of Cesium Lead Halide Perovskites (CsPbX3, X = Cl, Br, and I): Novel Optoelectronic Materials Showing Bright Emission with Wide Color Gamut," Nano Lett, vol. 15, no. 6, pp. 3692–3696, Jun. 2015, doi: 10.1021/nl5048779.
[31] S. Ullah et al., "All-inorganic CsPbBr3perovskite: A promising choice for photovoltaics," Jan. 21, 2021, Royal Society of Chemistry. doi: 10.1039/d0ma00866d.
[32] J. Chen, D. Liu, M. J. Al-Marri, L. Nuuttila, H. Lehtivuori, and K. Zheng, "Photo-stability of CsPbBr3 perovskite quantum dots for optoelectronic application," Sci China Mater, vol. 59, no. 9, pp. 719–727, Sep. 2016, doi: 10.1007/s40843-016-5123-1.
[33] Z. Liang et al., "Shape-Controlled Synthesis of All-Inorganic CsPbBr3Perovskite Nanocrystals with Bright Blue Emission," ACS Appl Mater Interfaces, vol. 8, no. 42, pp. 28824–28830, Oct. 2016, doi: 10.1021/acsami.6b08528.
[34] J. Liu et al., "Synthesis and optical applications of low dimensional metal-halide perovskites," Nanotechnology, vol. 31, no. 15, p. 152002, Apr. 2020, doi: 10.1088/1361-6528/ab5a19.
[35] L. Zhang, Y. Zhang, W. He, H. Peng, and Q. Dai, "CsPbBr3 perovskite nanowires and their optical properties," Opt Mater (Amst), vol. 109, Nov. 2020, doi: 10.1016/j.optmat.2020.110399.
[36] L. Rao et al., "CsPbBr3/Cs4PbBr6 heterostructure solids with high stability and photoluminescence for white light-emitting diodes," J Alloys Compd, vol. 919, Oct. 2022, doi: 10.1016/j.jallcom.2022.165857.
[37] S. Suresh, M. R. Subramaniam, S. Hazra, B. N. Pal, and S. K. Batabyal, "Solvent Evaporation Induced Large-Scale Synthesis of Cs4PbBr6 and CsPbBr3 Microcrystals: Optical Properties and Backlight Application for LEDs," ACS Omega, vol. 8, no. 5, pp. 4616–4626, Feb. 2023, doi: 10.1021/acsomega.2c05862.
[38] Y. M. Chen et al., "Cs4PbBr6/CsPbBr3 Perovskite Composites with Near-Unity Luminescence Quantum Yield: Large-Scale Synthesis, Luminescence and Formation Mechanism, and White Light-Emitting Diode Application," ACS Appl Mater Interfaces, vol. 10, no. 18, pp. 15905–15912, May 2018, doi: 10.1021/acsami.8b04556.
[39] F. Cao, D. Yu, X. Xu, Z. Han, and H. Zeng, "CsPbBr3@Cs4PbBr6Emitter-in-Host Composite: Fluorescence Origin and Interphase Energy Transfer," Journal of Physical Chemistry C, vol. 125, no. 1, pp. 3–19, Jan. 2021, doi: 10.1021/acs.jpcc.0c08100.
[40] O. F. Mohammed, "Outstanding Challenges of Zero-Dimensional Perovskite Materials," Oct. 03, 2019, American Chemical Society. doi: 10.1021/acs.jpclett.9b00175.
[41] S. Seth and A. Samanta, "Fluorescent Phase-Pure Zero-Dimensional Perovskite-Related Cs4PbBr6 Microdisks: Synthesis and Single-Particle Imaging Study," Journal of Physical Chemistry Letters, vol. 8, no. 18, pp. 4461–4467, Sep. 2017, doi: 10.1021/acs.jpclett.7b02100.
[42] J. H. Cha et al., "Superparamagnetism of Green Emissive Cs4PbBr6Zero-Dimensional Perovskite Crystals," ACS Energy Lett, vol. 5, no. 7, pp. 2208–2216, Jul. 2020, doi: 10.1021/acsenergylett.0c00964.
[43] L. Wang, H. Liu, Y. Zhang, and O. F. Mohammed, "Photoluminescence Origin of Zero-Dimensional Cs4PbBr6 Perovskite," ACS Energy Lett, vol. 5, no. 1, pp. 87–99, Jan. 2020, doi: 10.1021/acsenergylett.9b02275.
[44] M. Hu, C. Ge, J. Yu, and J. Feng, "Mechanical and Optical Properties of Cs4BX6 (B = Pb, Sn; X = Cl, Br, I) Zero-Dimension Perovskites," Journal of Physical Chemistry C, vol. 121, no. 48, pp. 27053–27058, Dec. 2017, doi: 10.1021/acs.jpcc.7b10629.
[45] H. Zhang, Q. Liao, Y. Wu, J. Chen, Q. Gao, and H. Fu, "Pure zero-dimensional Cs4PbBr6 single crystal rhombohedral microdisks with high luminescence and stability," Physical Chemistry Chemical Physics, vol. 19, no. 43, pp. 29092–29098, 2017, doi: 10.1039/c7cp06097a.
[46] X. Chen et al., "Centimeter-Sized Cs4PbBr6 Crystals with Embedded CsPbBr3 Nanocrystals Showing Superior Photoluminescence: Nonstoichiometry Induced Transformation and Light-Emitting Applications," Adv Funct Mater, vol. 28, no. 16, Apr. 2018, doi: 10.1002/adfm.201706567.
[47] W. A. Dunlap-Shohl, Y. Zhou, N. P. Padture, and D. B. Mitzi, "Synthetic Approaches for Halide Perovskite Thin Films," Chem Rev, vol. 119, no. 5, pp. 3193–3295, Mar. 2019, doi: 10.1021/acs.chemrev.8b00318.
[48] G. C. Adhikari, S. Thapa, H. Zhu, A. Grigoriev, and P. Zhu, "Synthesis of CsPbBr3 and Transformation into Cs4PbBr6 Crystals for White Light Emission with High CRI and Tunable CCT," Journal of Physical Chemistry C, vol. 123, no. 18, pp. 12023–12028, May 2019, doi: 10.1021/acs.jpcc.9b03369.
[49] R. Chairil, A. P. Forsberg, R. L. Brutchey, and N. Malmstadt, "High-throughput reaction discovery for Cs-Pb-Br nanocrystal synthesis," React Chem Eng, Nov. 2024, doi: 10.1039/d4re00491d.
[50] C. H. Lu, Y. H. Liu, M. L. Meena, and S. Som, "Synthesis and spectroscopic characterization of CsPbBr3/Cs4PbBr6 perovskites synthesized via the microwave-assisted heating process for backlight display devices," Org Electron, vol. 91, Apr. 2021, doi: 10.1016/j.orgel.2021.106079.

[51] Z. Bao et al., "Highly Luminescent CsPbBr3@Cs4PbBr6Nanocrystals and Their Application in Electroluminescent Emitters," Journal of Physical Chemistry Letters, vol. 11, no. 23, pp. 10196–10202, Dec. 2020, doi: 10.1021/acs.jpclett.0c03142.
[52] F. A. La Porta and S. Masi, "Solvent-Mediated Structural Evolution Mechanism from Cs4PbBr6 to CsPbBr3 Crystals," Nanomanufacturing, vol. 1, no. 2, pp. 67–74, Jul. 2021, doi: 10.3390/nanomanufacturing1020007.
[53] X. Peng, J. Chen, F. Wang, C. Zhang, and B. Yang, "One-pot synthesis of CsPbBr3/Cs4PbBr6 perovskite composite," Optik (Stuttg), vol. 208, Apr. 2020, doi: 10.1016/j.ijleo.2020.164579.
[54] C. Y. Huang, S. H. Huang, C. L. Wu, Z. H. Wang, and C. C. Yang, "Cs4PbBr6/CsPbBr3Nanocomposites for All-Inorganic Electroluminescent Perovskite Light-Emitting Diodes," ACS Appl Nano Mater, vol. 3, no. 12, pp. 11760–11768, Dec. 2020, doi: 10.1021/acsanm.0c02274.
[55] Z. Bao et al., "Efficient Luminescence from CsPbBr3Nanoparticles Embedded in Cs4PbBr6," Journal of Physical Chemistry Letters, vol. 11, no. 18, pp. 7637–7642, Sep. 2020, doi: 10.1021/acs.jpclett.0c02321.
[56] C. T. Altaf, N. Abdullayeva, M. Sankir, and N. D. Sankir, "CsPbBr3 and Cs4PbBr6–CsPbBr3 composite perovskite sensitization of 3D-ZnO nanostructures for enhanced photoluminescence emission," J Lumin, vol. 239, Nov. 2021, doi: 10.1016/j.jlumin.2021.118396.
[57] Z. Wang et al., "High Stability and Strong Luminescence CsPbBr3/Cs4PbBr6 Perovskite Nanocomposite: Large-Scale Synthesis, Reversible Luminescence, and Anti-Counterfeiting Application," Adv Mater Technol, vol. 6, no. 12, Dec. 2021, doi: 10.1002/admt.202100654.
[58] A. F. V. da Fonseca, B. R. C. Vale, T. A. de S. Carvalho, J. Bettini, A. C. Pereira, and M. A. Schiavon, "Charge Transfer Improvement after Solvent-Induced Phase Change in Type-I Cs4PbBr6@CsPbBr3 Core–Shell Perovskites," Journal of Physical Chemistry C, vol. 125, no. 49, pp. 27363–27371, Dec. 2021, doi: 10.1021/acs.jpcc.1c08102.
[59] C. H. Lu, Y. H. Liu, M. L. Meena, and S. Som, "Synthesis and spectroscopic characterization of CsPbBr3/Cs4PbBr6 perovskites synthesized via the microwave-assisted heating process for backlight display devices," Org Electron, vol. 91, Apr. 2021, doi: 10.1016/j.orgel.2021.106079.
[60] Q. He, E. Mei, X. Liang, and W. Xiang, "Ultrastable PVB films-protected CsPbBr3/Cs4PbBr6 perovskites with high color purity for nearing Rec. 2020 standard," Chemical Engineering Journal, vol. 419, Sep. 2021, doi: 10.1016/j.cej.2021.129529.
[61] V. Naresh, T. Jang, Y. Pang, and N. Lee, "Highly luminescent dual-phase CsPbBr3/Cs4PbBr6 microcrystals for a wide color gamut for backlight displays," Nanoscale, vol. 14, no. 47, pp. 17789–17801, Nov. 2022, doi: 10.1039/d2nr05653d.
[62] H. Babeker et al., "Preparation and photoluminescence properties of perovskite Cs4PbBr6/CsPbBr3 quantum dots integrated into lithium-borosilicate glass," Ceram Int, vol. 49, no. 15, pp. 24824–24830, Aug. 2023, doi: 10.1016/j.ceramint.2023.05.008.
[63] S. Ming, H. Chen, J. Huang, M. Li, B. Wang, and J. Su, "Solution preparation of CsPbBr3/Cs4PbBr6 polycrystalline composites," Physica B Condens Matter, vol. 647, Dec. 2022, doi: 10.1016/j.physb.2022.414378.
[64] D. Qian et al., " Mechanosynthesis strategy towards a high-efficiency CsPbBr 3 /Cs 4 PbBr 6 perovskite phosphor ," Opt Mater Express, vol. 12, no. 2, p. 665, Feb. 2022, doi: 10.1364/ome.448204.
[65] L. Rao et al., "Highly Stable and Photoluminescent CsPbBr3/Cs4PbBr6 Composites for White-Light-Emitting Diodes and Visible Light Communication," Nanomaterials, vol. 13, no. 2, Jan. 2023, doi: 10.3390/nano13020355.
[66] W. Sun, Y. T. Hung, W. T. Huang, R. S. Liu, and W. Zhou, "Photoluminescent Nano-CsPbBr3 Embedded in Cs4PbBr6 Crystals: Formation Mechanism and Properties," Cryst Growth Des, vol. 24, no. 1, pp. 545–553, Jan. 2024, doi: 10.1021/acs.cgd.3c01226.
[67] C. Wang, L. Yan, J. Si, T. Huo, and X. Hou, "Strongly luminescent and highly stable CsPbBr3/Cs4PbBr6 core/shell nanocrystals and their ultrafast carrier dynamics," J Alloys Compd, vol. 946, Jun. 2023, doi: 10.1016/j.jallcom.2023.169272.
[68] Q. Wang, S. K. Abkenar, M. Cirignano, H. Yu, W. Wu, and G. Divitini, "Temperature-dependent photoluminescent behavior of millimeter-scale Cs4PbBr6/CsPbBr3 bulk crystals and their application to white light-emitting diodes," J Mater Sci Technol, vol. 179, pp. 57–65, Apr. 2024, doi: 10.1016/j.jmst.2023.08.061.
[69] M. Jeong et al., "Stable perovskite solar cells with efficiency exceeding 24.8% and 0.3-V voltage loss." [Online]. Available: https://www.science.org
[70] B. Chen, P. N. Rudd, S. Yang, Y. Yuan, and J. Huang, "Imperfections and Their Passivation in Halide Perovskite Solar Cells."
[71] J. Zhu et al., "Phase Control of Cs-Pb-Br Derivatives to Suppress 0D Cs4PbBr6 for High-Efficiency and Stable All-Inorganic CsPbBr3 Perovskite Solar Cells," Small, vol. 18, no. 8, Feb. 2022, doi: 10.1002/smll.202106323.
[72] E. Darwish, J. Elia, A. Barabash, H. Hu, M. Batentschuk, and A. Osvet, "Modified Synthesis of Cs4PbBr6 for Enhanced Purity and Quantum Yield and for Exploring Its Potential as a High Stokes Shift Material for Down-Conversion in Solar Cells," Adv Eng Mater, Sep. 2024, doi: 10.1002/adem.202400082.
[73] J. X. Cao et al., "Perovskite solar cell with improved performance passivated by all inorganic perovskite quantum dots," in Journal of Physics: Conference Series, IOP Publishing Ltd, Apr. 2021. doi: 10.1088/1742-6596/1885/2/022019.
[74] J. Song et al., "Performance Enhancement of Crystal Silicon Solar Cell by a CsPbBr3–Cs4PbBr6 Perovskite Quantum Dot @ZnO/Ethylene Vinyl Acetate Copolymer Downshifting Composite Film," Solar RRL, vol. 6, no. 11, Nov. 2022, doi: 10.1002/solr.202200336.
[75] W. Z. She et al., "Selective Detection of Folic Acid Using a Water-Stable Fluorescent CsPbBr3/Cs4PbBr6 Perovskite Nanocrystal Probe," Chemosensors, vol. 11, no. 1, Jan. 2023, doi: 10.3390/chemosensors11010019.
[76] Y. Chen et al., "Reversible hydrochromic CsPbBr3/Cs4PbBr6@MCM-41 to enable organic solvent polarity detection," Chemical Engineering Journal, vol. 481, Feb. 2024, doi: 10.1016/j.cej.2024.148600.
[77] Y. Wang et al., "All-Inorganic CsPbBr3/Cs4PbBr6 Perovskite/ZnO for Detection of NO with Enhanced Response and Low-Work Temperature," ChemistrySelect, vol. 6, no. 36, pp. 9657–9662, Sep. 2021, doi: 10.1002/slct.202102051.
[78] Z. Wang et al., "High Stability and Strong Luminescence CsPbBr3/Cs4PbBr6 Perovskite Nanocomposite: Large-Scale Synthesis, Reversible Luminescence, and Anti-Counterfeiting Application," Adv Mater Technol, vol. 6, no. 12, Dec. 2021, doi: 10.1002/admt.202100654.
[79] L. Xu et al., "Double-Protected All-Inorganic Perovskite Nanocrystals by Crystalline Matrix and Silica for Triple-Modal Anti-Counterfeiting Codes," ACS Appl Mater Interfaces, vol. 9, no. 31, pp. 26556–26564, Aug. 2017, doi: 10.1021/acsami.7b06436.
[80] S. S. Revankar et al., "Fluorescent CsPbBr3@Cs4PbBr6/PU polymer nanocomposite-based triboelectric nanogenerator for self-powered UV sensing," Mater Today Chem, vol. 44, Mar. 2025, doi: 10.1016/j.mtchem.2025.102601.
[81] Y. Han et al., "Photodetector based on CsPbBr3/Cs4PbBr6 composite nanocrystals with high detectivity," Crystals (Basel), vol. 11, no. 11, Nov. 2021, doi: 10.3390/cryst11111287.
[82] P. Qiu et al., "Fabricating Surface-Functionalized CsPbBr3/Cs4PbBr6 Nanosheets for Visible-Light Photocatalytic Oxidation of Styrene," Front Chem, vol. 8, Mar. 2020, doi: 10.3389/fchem.2020.00130.
[83] D. Gu et al., "Stability and photocatalytic performance enhancement of sodium-doped CsPbBr 3 /Cs 4 PbBr 6 nanocomposites for dye wastewater degradation," Phys Scr, vol. 99, no. 8, p. 085943, Aug. 2024, doi: 10.1088/1402-4896/ad5e0d.